International Journal of
INTELLIGENT SYSTEMS AND APPLICATIONS IN ENGINEERING
ISSN:2147-6799 www.ijisae.org Original Research Paper

# Spatial Filter Analysis for Speckle Reduction in Synthetic Aperture Radar Images

**Sushant Pawar*[1], Sanjay Gandhe[2]**

**Submitted**:12/03/2024 **Revised**: 27/04/2024 **Accepted**: 04/05/2024

**Abstract:** High-resolution Earth imagery can be captured with Synthetic Aperture Radar (SAR), a powerful tool that works in a variety of lighting and weather conditions. However, speckle noise distorts SAR images, making them less interpretable and of lower quality overall. Using speckle filtering becomes essential in the SAR image processing pipeline in order to protect important elements in these images. Speckle noise reduction significantly improves the overall quality and interpretability of SAR imagery. The literature has proposed a number of methods, including frequency domain filtering, multilooking, wavelet-based filtering, and spatial filtering. Every method has unique benefits and limitations, and the best filter option depends on the use cases and sensor capabilities. The efficacy of a speckle filter is determined by how well it reduces noise while maintaining image edges and fine details. Analysing filtered imagery guarantees that important details are preserved in addition to the desired noise reduction. Standard benchmarks for assessing speckle filter performance include peak signal-to-noise ratio (PSNR), normalised root mean square error (NRMSE), mean square error (MSE), and structural similarity index (SSIM). Speckle filtering, which improves image quality and makes interpretation simpler, is still, in essence, an essential step in the processing of SAR images. Sentinel SAR imagery is used to support qualitative and quantitative analyses of spatial filters for efficient speckle reduction.

***Keywords:*** *Multilooking, ENL, Sentinel SAR, Spatial Filters, Statistical Analysis*

## 1. Introduction

Synthetic Aperture Radar (SAR) is used for remote sensing in many industries, including forestry, agriculture, geology, oceanography, and military applications. Regardless of the lighting or weather, this technology provides high-resolution Earth surface data, providing insights that are difficult to obtain through optical imaging techniques. The fidelity of SAR data collection is maintained in a variety of weather conditions, at night and during the day, and even in the presence of smoke or haze.

SAR images are produced by both airborne and space-based sensors, but their quality can be affected by noise and distortion, which affects interpretation. For the purpose of deriving meaningful insights from these images, efficient SAR image processing is therefore necessary. The issues of noise and distortion must be resolved in order to extract accurate and significant information from SAR data for a variety of sectors and applications [1].

To improve the quality of SAR images, processing aims to reduce noise and distortion, increase resolution, and extract useful information. The methods used in SAR image processing include segmentation, filtering, registration, feature extraction, and classification. By enhancing the quality and interpretability of SAR images, these techniques hope to facilitate better decision-making in a range of applications. In the end, the processing aims to improve SAR images by making them sharper, more detailed, and easier to extract useful information for a variety of applications [2].

Speckle, a granular noise pattern in SAR images, is frequently introduced by the intrinsic coherence and multiplicative aspects of radar signals. In addition to severely reducing the visual quality of SAR images, this speckle noise also affects the precision of subsequent image analysis tasks such as object detection, classification, and segmentation. As a result, as was already mentioned, speckle reduction in SAR images has emerged as a crucial first step for many applications. A variety of techniques, from traditional filters to state-of-the-art deep learning methods, are used to address this problem. This paper explores these methods of speckle reduction and presents advances in classical filters through quantitative and qualitative statistical analyses. Moreover, it delves into the field of speckle reduction in SAR images acquired from sentinel platforms, contributing to a more comprehensive understanding of this vital image enhancement procedure [3].

## 2. Review History

In recent years, several techniques have been proposed to address the speckle issue. Sentinel -1A & Sentinel 1-B SAR image data has to follow some specified pre-processing steps, including orbit correction, subset creation, thermal noise correction, radiometric calibration, range doppler

[1] *Sandip Institute of Tech & Research Centre, Nashik – 422213, India*
*Pune Institute of Computer Technology, Pune – 411043, India*
*ORCID ID: 0000-0002-9992-9498*
[2] *Pune Institute of Computer Technology, Pune – 411043, India*
*ORCID ID: 0009-0003-2236-3865*
** Corresponding Author Email: pawar.sushant@gmail.com*

terrain corrections. This depends on the specific application & types of images acquired by the sensors [19].

In this review, we provide an overview of some of the most commonly used speckle reduction techniques for SAR image data.

Deep learning techniques have demonstrated promising results in the area of speckle reduction in SAR images. Through the use of deep neural networks, these methods are able to grasp intricate relationships between noisy and clean images, using patterns that have been learned to carry out denoising algorithms. This covers variations based on convolutional neural networks, generative adversarial networks, and variational autoencoders. Although these methods produce state-of-the-art results, they frequently require large amounts of training data and computational power to reach their maximum potential.

Most techniques used to reduce speckles in SAR images have their roots in wavelet technology. These techniques take advantage of wavelet transforms' multi-resolution properties and use thresholding to reduce noise while preserving fine details and image edges. These methods include the Bayesian wavelet shrinkage, cycle-spinning, and contourlet transform. Although wavelet-based techniques frequently produce excellent results, they can also introduce artifacts, so careful wavelet parameter selection is necessary to get the best outcomes [9].

The use of non-local means techniques to reduce speckle in SAR images has become increasingly popular in recent years. By comparing image patches, these techniques use a weighted averaging scheme to suppress noise and take advantage of the redundancy within the patches. These include the Block Matching and 3D filtering approach, the Non-Local Bayes method, and the Non-Local Means filter. Although these methods are excellent at maintaining subtle nuances and edges and frequently yield positive results, their use may require a significant amount of computational complexity [8].

Often used conventional filters like Lee, Frost, and boxcar filters are meant to reduce speckle in SAR images. These filters lessen the impact of speckle noise by using statistical features and local averaging. Although these filters are simple and efficient in terms of computation, they frequently have a tendency to smooth the output too much, which makes them less effective in maintaining image edges and fine details [3, 4, 8].

This paper focuses on the improved version of classical filter techniques for speckle reductions, which overcomes the basic limitations including, over smoothness, depressed strongly reflected objects, outlier suppression & detection. Results show the betterment of improved versions of classical methods over basic versions.

## 3. Input Dataset

Input image dataset is acquired sentinel-1A SAR sensors near to the Vishakhapatnam Indian coastal region, dual polarized dataset, the details are given in the table 1, & intensity VV image shown in the figure 1. Acquired SAR data includes land as well as sea portions, homogeneous as well as non-homogeneous areas of image data, hence we can observe the speckle distributions in both the regions & analyzed. As this SAR image data is unprocessed level-1 ground range data product (GRD), hence initial preprocessing on this data is requires, it includes, orbital correction, calibration, multi-looking, terrain correction, thermal correction, speckle filtering, deburst operations in case of for SCAN SAR image dataset, Sea- Land masking, depending on the end use & nature of the acquisition of source dataset [19].

**Table 1.** SAR Product details

| | |
|---|---|
| PRODUCT | S1A_IW_GRDH_1SDV_20190219T002214_20190219T002239_025991_02E566_A3C0 |
| PRODUCT_TYPE | GRD |
| SPH_DESCRIPTOR | Sentinel-1 IW Level-1 GRD Product |
| MISSION | SENTINEL-1A |
| ACQUISITION_MODE | IW (interferometric wide) |
| antenna pointing | right |
| orbit cycle | 163 |
| incidence near | 30.8417654 |
| incidence far | 46.17062759 |
| PASS | DESCENDING |
| POLARIZATION | VV+VH |
| azimuth looks | 1 |
| range looks | 5 |
| range spacing | 10 |
| azimuth spacing | 10 |
| Pulse repetition frequency | 1717.12897387803 HZ |
| radar frequency | 5405.00045433434 MHZ |
| RASTER HEIGHT | 6881 (16756) |
| RASTER WIDTH | 5333 (25514) |

The acquired dataset is GRD product, hence preprocessing includes orbital correction. Several regions including luminance extraction, gravitational force, and various atmospheric drag satellites do not follow their designated path & hence we require orbit correction. The orbit file provides accurate satellite position and velocity information. Based on this information, the orbit state vectors in the abstracted metadata of the product are updated. Orbit file available days-to-weeks after the generation of the product from ESA GNSS Hub to refine the

state vectors. Visually we cannot separate the orbital corrected image from the input.

As the size of the acquired dataset is very large to process, hence subset operation on the source dataset is required for the area of interest. Figure 2 shows the subset version of the source dataset which considered land as well as sea for speckle analysis. This is a range-doppler terrain corrected intensity image dataset. Followed by thermal noise correction [10] & radiometric calibration.

Thermal noise increases the density of dark objects from actual. Hence correction & removal of thermal noise is required to normalize the backscatter signal within the entire image. Thermal noise index is calculated using the following equation 1, which decides the intensity of thermal noise.

$$N_{\sigma} = n_r + 30\log\left(\frac{r_s}{r}\right) - 2 * G_r + 10 * \log\left(\sin\left(I\right)\right) \quad (1)$$

For this we need, Noise reference level ($n_r$), Slant Range ($r_s$), reference range (r), Antenna Pattern correction ($G_r$) and incidence angle (I). This can be taken from metadata provided with the SAR data.

**Fig. 1.** Sentinel SAR Level-1 GRD Source Image near Visakhapatnam, India.

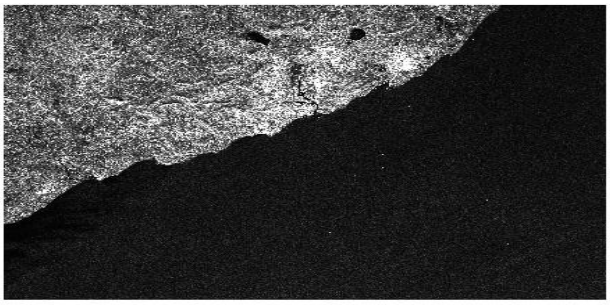

**Fig. 2**. Subset Intensity VV polarized SAR

Radiometric calibration calibrates the input data and generate the backscatter sigma nought ($\sigma_o$) Images. Calibration is required to represent the actual value of backscatter from reflecting objects i.e., the imagery in which the pixel value directly represents the radar backscatter of the object. Level -1 data set generally not radiometrically calibrated. Hence for quantitative use of SAR data calibration is required [20].

**4. Speckle Noise**

Inherent problem in SAR image data is the speckle. Also called coherent noise or speckle noise. Speckle noise can be defined as the interference of unwanted signals added in phase & hence added gray parts in the SAR image called speckle. In the Speckle affected SAR image, the resolution cell appears larger and brighter than usual. hence false alarm rate increases. Speckle, which is caused by the presence of many elementary scatterers with random distributions within the resolution cell. The total complex reflectivity [1] for each resolution cell expressed in equation 2.

$$\varphi = \sum i\sqrt{\sigma_i}\,\exp\left(i\varphi_i scatt\right) * \exp\left(-i\frac{4\pi}{\lambda}r_0, i\right) \quad (2)$$

Where ***i,*** is the number of elemental scatterers within the resolution cell, $\varphi_i Scatt$ is the scattering phase, $\sigma_i$ is the backscattering RCS coefficient, $r_0$ is the distance from antenna to the target.

The cell where constructive interference dominates will appear to have high reflectivity, and where destructive interference dominates will appear to have a low reflectivity. This may lead that the intensity & phase in the final image are no longer deterministic. This affects the measurement qualitatively as well as quantitatively.

Speckle reduction follows mainly two techniques, one is noncoherent averaging of the intensity image, as a result, improves the image interpretability though it causes the degradation in the image resolution. This technique is called multilook operation. Multilooking makes sense when handling the returns from the same scene or target. SAR images have distributed multiple object echoes, hence the multilook averaging does not make sense. Another approach is adaptive image restoration techniques i.e., post image formation methods it includes classical filtering methods.

**5. Speckle Index**

As we know that removal of speckle may lose some features or cause the degradation of image features, hence we need some parameter for deciding the type of speckle distribution & type of speckle filtering technique required. This measurement is known as speckle index calculation. Instead, speckle intensity has a uniform and exponential distribution; despite this, speckle behaves differently, and we may calculate its average value. The speckle index parameter, N shows the what type of distribution speckle have, where this N is defined as in equation 3.

$$ENL = N = \frac{\mu^2}{v} = \frac{1}{VMR}, \quad \lambda = \frac{v}{\mu} \quad (3)$$

With N is a speckle index or shape parameter and $\lambda$ is the scale parameter. $\mu$ is the mean & v is the Variance and VMR is the variance to mean ratio. ENL called expected or equivalent number of looks, which indicate how many indents measurement of a pixel is based on, which indicate the speckle strength in SAR Image [21, 6].

From figure 3 intensity follows the exponential, gamma & gaussian distributions. As N increases, the distribution follows the gaussian distribution. For homogeneous regions the distribution follows the gamma distribution. Large numbers of ENL means weaker speckles.

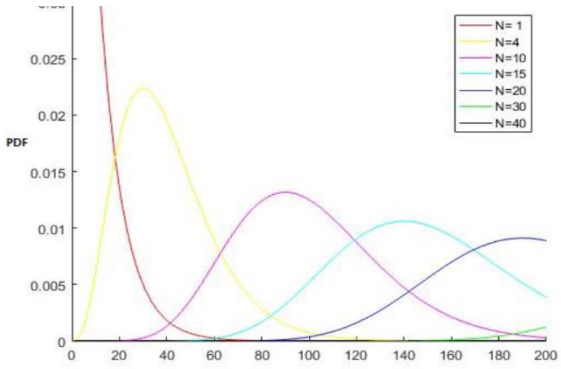


**Fig. 3.** Distribution of different shape parameter N

## 6. Statistical Analysis

For statistical analysis of speckles present in the input source data, we divided the source data into seven different segments, which includes homogeneous & nonhomogeneous areas from land & sea portion. Figure 4 shows the input source data with different regions of interest.

Region 1 will be the bright field, intensity is very high, region 2, 6 & 7 is the ocean region, which is a homogeneous area, it looks dark with very low intensity. Region 3 is the mix area which includes the dark area surrounded by the bright field & region 4 is the coastline field which includes the land & sea area both are clearly separated by an edge between them. Region 5 & 8 are sea areas but nonhomogeneous. Figure 5 shows the log intensity distributions of the eight regions respectively. Table 2 shows the statistical analysis of selected regions.

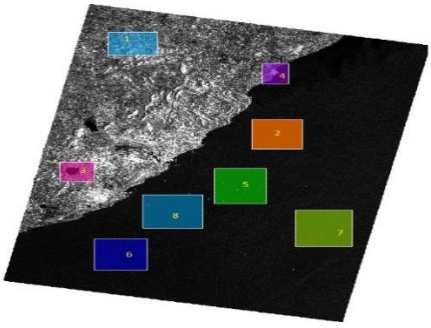

**Fig. 4.** Sentinel-1 Level-1 GRD unfiltered image divided into seven regions.

It is observed that except in regions 2, 6, & 7 the coefficient of variance is larger, hence their expected number of looks (ENL) is very small. The intensity distribution of region 2, 6, & 7 is almost similar. Hence speckle index of region 2, 6, 7 are larger compared to others, no need to apply speckle filter. rest regions are required to apply filtering.

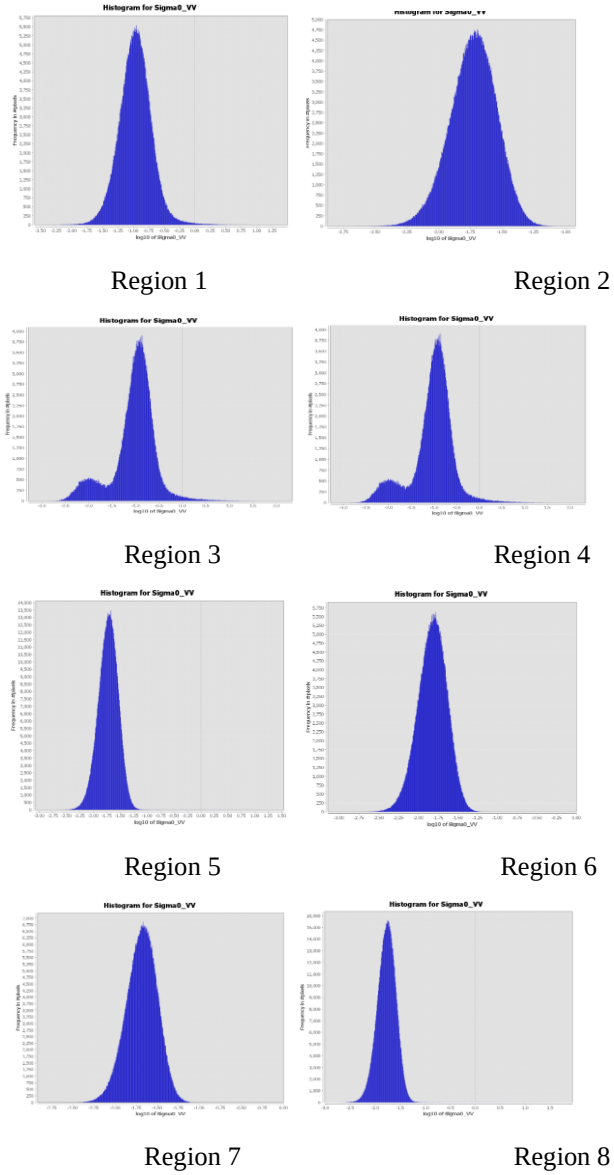


**Fig. 5.** Corresponding log intensity distributions of regions 1 to 8

**Table 2.** Statistics of corresponding regions (1-8)

| **Region 1** | | **Region 2** | |
|---|---|---|---|
| Number of pixels | 448941 | Number of pixels | 608936 |
| Mean | 0.1327 | Mean | 0.0204 |
| Sigma | 0.1552 | Sigma | 0.0085 |
| Median | 0.1081 | Median | 0.0190 |
| Coefficient variation | 1.1701 | Coefficient variation | 0.4162 |
| ENL | 0.7304 | ENL | 5.7710 |
| **Region 3** | | **Region 4** | |

| | | | |
|---|---|---|---|
| Number of pixels | 279379 | Number of pixels | 222208 |
| Mean | 0.1673 | Mean | 0.0657 |
| Sigma | 0.6391 | Sigma | 0.1185 |
| Median | 0.1064 | Median | 0.0161 |
| Coefficient variation | 3.8195 | Coefficient variation | 1.8031 |
| ENL | 0.0685 | ENL | 0.3076 |
| **Region 5** | | **Region 6** | |
| Number of pixels | 736716 | Number of pixels | 666264 |
| Mean | 0.0223 | Mean | 0.0163 |
| Sigma | 0.1060 | Sigma | 0.0068 |
| Median | 0.0183 | Median | 0.0153 |
| Coefficient variation | 4.7522 | Coefficient variation | 0.4178 |
| ENL | 0.0443 | ENL | 5.7266 |
| **Region 7** | | **Region 8** | |
| Number of pixels | 830700 | Number of pixels | 804130 |
| Mean | 0.0225 | Mean | 0.0205 |
| Sigma | 0.0094 | Sigma | 0.1902 |
| Median | 0.0210 | Median | 0.0120 |
| Coefficient variation | 0.4204 | Coefficient variation | 9.2672 |
| ENL | 5.6572 | ENL | 0.0116 |

Figure 6 shows the bar graph of corresponding regions ENL.

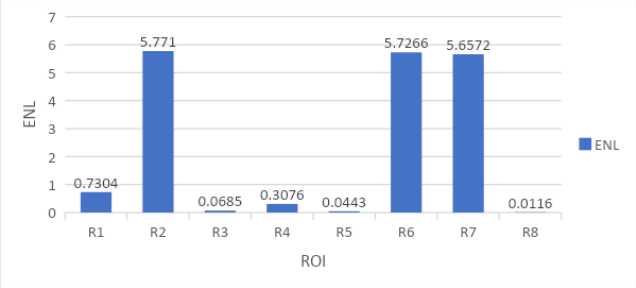


**Fig. 6.** ENL for the different region of interest for VV Image

## 7. Filter Analysis

The most commonly used classical filters are, boxcar filter, median filter, froast filter [11] gamma map filter [12,13], Lee filter & refined lee filter [14, 5], Lee sigma filter [15,7], Improved dark channel with its variants filter. These basic classical filters need to improve based on the type of speckle distribution with the different window size

For analysis of filters considered region 4 and applied various filters for improvement of expected number of looks while reducing the speckle in the image. The following figure 7 shows the corresponding visual results of filter outputs.

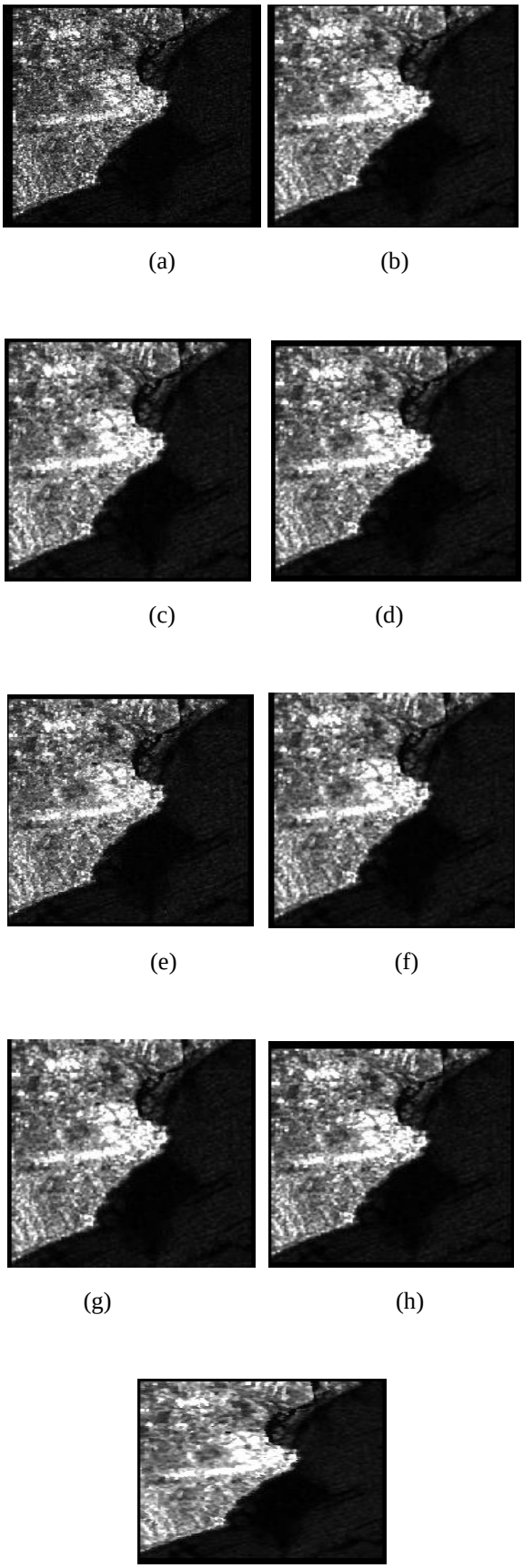


**Fig. 7.** (a) Original Image, (b)Boxcar, (c)Median, (d) Frost, (e) Gamma Map, (f) Lee, (g) Refined Lee, (h) Lee sigma, (i) IDAN All filters with 5x5 kernel

The qualitative analysis of the filtering process is shown in the table 3 below, this shows the expected number of looks (ENL) which is a measure of speckle noise in the image. from this table it shows a significant improvement in the speckled image. Median filter & refined lee filter shows the improvement in the ENL. At the same time, we also take care that edges should be preserved. From table 4 quantitative analysis [16, 17, 18, 22] of filters shows that as compared to all other filters, refined lee filters show significant improvement in the speckle noise while preserving the edges.

**Table 3.** Qualitative analysis of filters region 4

| Filters | Expected Number of looks (ENL) |
|---|---|
| Original Geometry_4 | 0.3085 -with speckle |
| Boxcar | 0.5705 |
| Median | 0.7384 |
| Frost | 0.4474 |
| Gamma Map | 0.5736 |
| Lee | 0.5728 |
| Refined Lee | 0.7821 |
| Lee sigma | 0.3347 |
| IDAN | 0.5192 |

**Table 4.** Quantitative analysis of filters region 4 [19][20][21]

| Filters | MSE | NRMSE | PSNR | SSIM |
|---|---|---|---|---|
| Boxcar | 0.0106 | 0.1377 | 19.7290 | 0.8846 |
| Median | 0.0106 | 0.1377 | 19.7286 | 0.8858 |
| Frost | 0.0063 | 0.1062 | 21.9858 | 0.9356 |
| Gamma Map | 0.0106 | 0.1376 | 19.7323 | 0.8847 |
| Lee | 0.0106 | 0.1377 | 19.7290 | 0.8846 |
| Refined Lee | 0.0034 | 0.0780 | 24.6691 | 0.9728 |
| Lee sigma | 0.0101 | 0.1340 | 19.9633 | 0.8872 |
| IDAN | 0.0136 | 0.1558 | 18.6569 | 0.8632 |

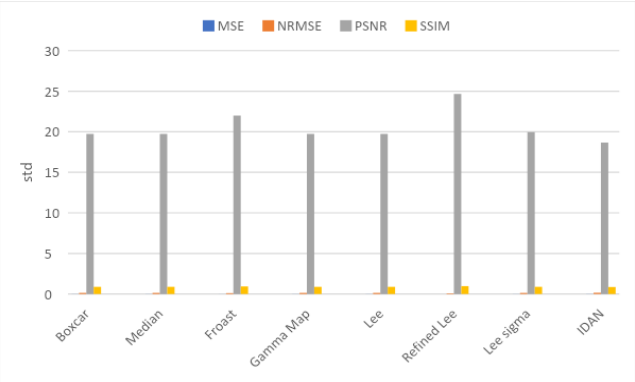


**Fig. 8.** Quantitative analysis of filters region 4

Figure 8 shows the bar graph of Quantitative analysis of region 4, it shows the refined lee filters have better performance over the rest.

Similarly, considered for region 5, only for the sea region, which is non homogeneous, and applied all filters for speckle reduction. The following figure 9 shows the visual results of all filters. from qualitative analysis from table 5 shows that combination of lee filters shows the significant result on most of the regions which include land see image data as shown in the region4, homogenous as well as nonhomogeneous regions. Also, from the quantitative results from table 6 shows the lee sigma filters give better results over all the classical filters with edge preserving ability.

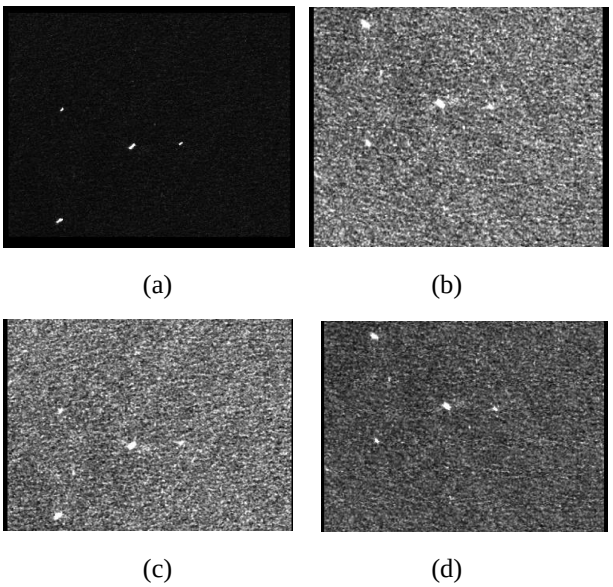

(a) (b)

(c) (d)

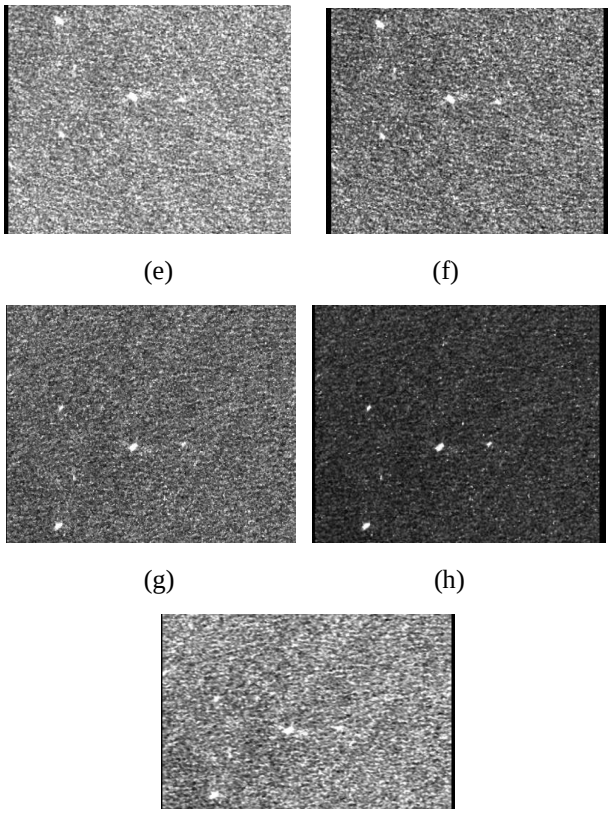

(e) (f)

(g) (h)

(i)

**Fig. 9**. (a) Original Image, (b)Boxcar, (c)Median, (d) Froast, (e) Gamma Map, (f) Lee, (g) Refined Lee, (h) Lee sigma, (i) IDAN All filters with 5x5 kernel.

**Table 5.** Qualitative analysis of filters region 5

| Filters | Expected Number of looks (ENL) |
|---|---|
| Original Geometry_5 | 0.442 |
| Boxcar | 0.0881 |
| Median | 0.1441 |
| Frost | 0.0722 |
| Gamma Map | 0.0872 |
| Lee | 0.0878 |
| Refined Lee | 0.0876 |
| Lee sigma | 0.2141 |
| IDAN | 0.0446 |

**Table 6.** Quantitative analysis of filters region 5 [19][20][21]

| Filters | MSE | NRMSE | PSNR | SSIM |
|---|---|---|---|---|
| Boxcar | 0.1570 | 0.5441 | 8.0411 | 0.3572 |
| Median | 0.1562 | 0.5426 | 8.0645 | 0.3549 |
| Froast | 0.1405 | 0.5147 | 8.5237 | 0.3992 |
| Gamma Map | 0.1890 | 0.5970 | 7.2350 | 0.3552 |
| Lee | 0.1585 | 0.5467 | 7.9990 | 0.3555 |
| Refined Lee | 0.1493 | 0.5306 | 8.2585 | 0.3492 |
| Lee sigma | 0.1485 | 0.5291 | 8.2836 | 0.4658 |
| IDAN | 0.1781 | 0.5795 | 7.4938 | 0.3691 |

From figure 10 observed that for homogeneous region froast filter and refined lee sigma filters give better performance over the rest. Concisely combination of Lee and Sigma filter is preferred solution of level 1 sentinel calibrated SAR image data.

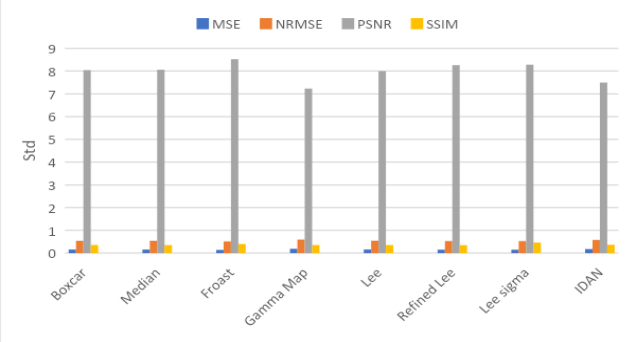


**Fig. 10.** Quantitative Analysis of filters for region 5

## 8. Conclusion

In conclusion, we have applied different classical filters on real time SAR data for various regions including land-sea portion, homogenous as well as non-homogeneous region of sea portion. From the results we observe that in speckle determination ENL plays a very important role which gives the speckle index from which we can determine the need for speckle filtering. The relation between ENL & speckle index (SI) is inversely proportional. when we apply a speckle filter, we need to take care about the edge preservation also else we lose the important target information. Keeping this in mind advanced versions of lee filters play a significant role for both speckle reduction with keeping structural similarity. Filter window size is also important for consideration as for homogenous regions we can consider the larger size over the non-homogenous regions. In further we need to check filters on SAR data


## Acknowledgments

I would like to thank Dr. Sanjay Gandhe, for their regular guidance, and also thankful to the scientists from the Indian Institute of Remote Sensing (IIRS) for their contribution to the field of remote sensing and for their insightful discussion on SAR data & related methodology.


## Conflicts of Interest

The author(s) declare(s) that there is no conflict of interest regarding the publication of this paper

**References**


[1] A. Moreira, P. Prats-Iraola, M. Younis, G. Krieger, I. Hajnsek, and K. P. Papathanassiou, "A tutorial on synthetic aperture radar," IEEE Geosci. Remote Sens. Mag., vol. 1, no. 1, pp. 6–43, 2013

[2] G. Gao, "Statistical modeling of SAR images: A survey," Sensors, vol. 10, no. 1, pp. 775–795, 2010

[3] J.-S. Lee, L. Jurkevich, P. Dewaele, P. Wambacq, and A. Oosterlinck, "Speckle filtering of synthetic aperture radar images: A review," Remote Sens. Rev., vol. 8, no. 4, pp. 313–340, 1994

[4] C. Ju and C. Moloney, "An Edge-Enhanced Modified Lee Filter for the Smoothing of SAR Image Speckle Noise"

[5] J.-S. Lee, "Refined filtering of image noise using local statistics," Comput. Graph. Image Process., vol. 15, no. 4, pp. 380–389, 1981.

[6] F. Argenti, A. Lapini, T. Bianchi, and L. Alparone, "A tutorial on speckle reduction in synthetic aperture radar images," IEEE Geosci. Remote Sens. Mag., vol. 1, no. 3, pp. 6–35, 2013

[7] Jong-Sen Lee, Jen-Hung Wen, T. L. Ainsworth, Kun-Shan Chen, and A. J. Chen, "Improved Sigma Filter for Speckle Filtering of SAR Imagery," IEEE Trans. Geosci. Remote Sens., vol. 47, no. 1, pp. 202–213, Jan. 2009, doi: 10.1109/TGRS.2008.2002881

[8] L. Torres, S. J. S. Sant'Anna, C. da Costa Freitas, and A. C. Frery, "Speckle reduction in polarimetric SAR imagery with stochastic distances and nonlocal means," Pattern Recognit., vol. 47, no. 1, pp. 141–157, Jan. 2014, doi: 10.1016/j.patcog.2013.04.001.

[9] A. Alam and A. Rai, "Reduction of Speckle Noise in SAR Images With Hybrid Wavelet Filter".

[10] J.-W. Park, A. Korosov, and M. Babiker, "Efficient thermal noise removal of Sentinel-1 image and its impacts on sea ice applications," p. 12613, Apr. 2017.

[11] V. S. Frost, J. A. Stiles, K. S. Shanmugan, and J. C. Holtzman, 'A model for radar images and its application to adaptive digital filtering of multiplicative noise', IEEE Trans. Pattern Anal. Mach. Intell., no. 2, pp. 157–166, 1982.

[12] A. Baraldi and F. Parmiggiani, 'A refined gamma MAP SAR speckle filter with improved geometrical adaptivity', IEEE Trans. Geosci. Remote Sens., vol. 33, no. 5, pp. 1245–1257, Sep. 1995, doi: 10.1109/36.469489

[13] M. Beauchemin, K. P. B. Thomson, and G. Edwards, 'Optimization of the Gamma-Gamma MAP filter for SAR image clutters', Int. J. Remote Sens., vol. 17, no. 5, pp. 1063–1067, Mar. 1996, doi: 10.1080/01431169608949067

[14] C. Ju and C. Moloney, 'An Edge-Enhanced Modified Lee Filter for the Smoothing of SAR Image Speckle Noise'

[15] Jong-Sen Lee, Jen-Hung Wen, T. L. Ainsworth, Kun-Shan Chen, and A. J. Chen, 'Improved Sigma Filter for Speckle Filtering of SAR Imagery', IEEE Trans. Geosci. Remote Sens., vol. 47, no. 1, pp. 202–213, Jan. 2009, doi: 10.1109/TGRS.2008.2002881

[16] N. Biradar, M. L. Dewal, M. Rohit, S. Gowre, and Y. Gundge, 'Blind Source Parameters for Performance Evaluation of Despeckling Filters', Int. J. Biomed. Imaging, vol. 2016, pp. 1–12, 2016, doi: 10.1155/2016/3636017

[17] J. L. Mateo and A. Fernández-Caballero, 'Finding out general tendencies in speckle noise reduction in ultrasound images', Expert Syst. Appl., vol. 36, no. 4, pp. 7786–7797, May 2009, doi: 10.1016/j.eswa.2008.11.029.

[18] M. Mansourpour, M. A. Rajabi, and J. A. R. Blais, 'Effects and Performance of Speckle Noise Reduction Filters on Active Radar and SAR Images'.

[19] F. Filipponi, "Sentinel-1 GRD Preprocessing Workflow," in 3rd International Electronic Conference on Remote Sensing, MDPI, Jun. 2019, p. 11. doi: 10.3390/ECRS-3-06201.

[20] K. El-Darymli, P. McGuire, E. Gill, D. Power, and C. Moloney, "Understanding the significance of radiometric calibration for synthetic aperture radar imagery," in 2014 IEEE 27th Canadian Conference on Electrical and Computer Engineering (CCECE), IEEE, 2014, pp. 1–6.

[21] Y. Yan, Y. Zhou, and C.-S. Li, "Quantitative assessment of speckle filters for SAR images," in Second International Conference on Image and Graphics, SPIE, 2002, pp. 428–433

[22] Y. Yan, Y. Zhou, and C.-S. Li, 'Quantitative assessment of speckle filters for SAR images', in Second International Conference on Image and Graphics, SPIE, 2002, pp. 428–433